Bistable defect systems in $CdF_2 : M^{3+}$ (M = Al, Ga, In) and their photorefractive properties

1997 J. Phys.: Condens. Matter 9 3575

(http://iopscience.iop.org/0953-8984/9/17/007)

J. Phys.: Condens. Matter **9** (1997) 3575–3581. Printed in the UK PII: S0953-8984(97)79479-7

Bistable defect systems in CdF_2:M^{3+} (M = Al, Ga, In) and their photorefractive properties

Chun-rong Fu and K S Song

Physics Department, University of Ottawa, Ottawa, Ont., Canada K1N 6N5

Received 12 November 1996

Abstract. On the basis of the method recently used in the study of the trivalent impurity state in CdF_2:M^{3+} (M: In, Ga, Sc and Y), the structure of the electron trapped at an Al^{3+} centre in CdF_2 is determined. Although a bistable system is obtained, due to the locally soft lattice around the Al^{3+} ion the localized compact state has higher energy than the delocalized state. The excited p-like states and the oscillator strengths for the optical transition between the s- and p-like states in the three bistable systems (with Al, Ga, In) are evaluated. The changes in the refractive index as the systems change from localized to delocalized states are estimated, and the results are discussed in the context of the recently reported data on the photorefractive properties of In and Ga centres in CdF_2.

1. Introduction

The study of the bistable defect system in semiconducting CdF_2 crystals doped with In and Ga impurities has drawn considerable attention in the past two decades [1–4]. Most of the trivalent metals when doped into CdF_2 produce stable (or metastable) hydrogenic donor states [5]. The metals In [1] and Ga [3] have shown unusual bistable behaviour, i.e., the electrons can be trapped by the impurity either in a highly localized orbit or in a delocalized one separated by a vibronic barrier. The wavefunction of the former is very compact, while for the latter it is a diffuse and effective-mass-like one. At low temperature (below 70 K), a 200 meV barrier prevents the recovery to the ground state from the shallow hydrogenic state in CdF_2:In^{3+}. The photoionization of the two In states occurs in different spectral regions. At room temperature, two strongly asymmetric bands are seen [1]. The absorption band in the visible range ($\lambda < 650$ nm) is caused by the photoionization of the localized In^{2+} ground state, while the IR band, peaking at $\lambda \approx 8$ μm, is due to the photoionization of the hydrogenic, diffuse state of In^{3+}. The localized ground state is only 0.1 eV thermally deeper than the hydrogenic state, but it exhibits an enormous 2 eV Stokes shift. The shift is caused by a large lattice relaxation around the impurity occurring during photoionization [2, 4]. The resulting lattice collapse in the diffuse state is responsible for the 0.2 eV vibronic barrier separating the two In states and, hence, for the defect metastability. The absorption spectrum of CdF_2:Ga has similar asymmetric bands peaked at 4 eV and 0.17 eV [3], respectively. It is believed that Ga is a second bistable impurity centre in CdF_2.

On the basis of a simple configuration coordinate (cc) model, Cai and Song [4] presented a study of the M^{3+} (M = In, Ga, Sc, and Y) impurity with an excited electron bound to it. The discrete structure of the lattice and the detailed interaction between the excited electron

0953-8984/97/173575+07$19.50

and the impurity atom as well as the surrounding ions of Cd^{2+} and F^- were explicitly taken into account within the approach of the extended-ion method. In the crystals of CdF_2:In and CdF_2:Ga, as expected, the theoretical calculations exhibit a strongly relaxed lattice environment associated with the shallow (diffuse electron wavefunction) level, and an almost undistorted lattice environment for the deep (compact-state) level. The numerical results are in reasonable agreement with the experimental data of reference [3]. The absence of a deep level in Y and Sc centres was also predicted.

Recently, Ryskin *et al* [6] and Koziarska *et al* [7] reported on a successful holographic recording based on the bistable defect centres in CdF_2. They reported that a saturation value of about -1.3×10^{-4} was achieved in the refractive index change in the CdF_2:In at about 120 K, while the maximum of the diffraction efficiency occurs at about 280 K for Ga. Therefore, CdF_2:Ga crystals are apparently suitable for room temperature recording.

In this paper we first present a study of the defect centre in CdF_2:Al^{3+} by using the same approach as in reference [4]. Al is another trivalent metal, in the same column of the periodic table as In and Ga. But its deep core only contains two electrons ($1s^2$), and the radius of the ion Al^{3+} is much smaller than those of the other trivalent metals. Therefore, the short-range interaction between Al^{3+} and F^- is expected to be much weaker. With an impurity Al^{3+} ion replacing a Cd^{2+} ion, the ions surrounding the Al^{3+} are expected to undergo a large relaxation. Indeed quite different features are obtained in the structure of the system CdF_2:Al. We then proceed to evaluate the optical parameters connecting the ground states to the p-like excited states, and estimate the refractive index changes within the two-oscillator model [6, 7].

We will describe the methods used and the parameters for Al^{3+} in section 2, and then calculate the adiabatic potential energy surface (APES) of CdF_2:Al. Section 3 is devoted to the discussion of the excited-state properties of the bistable defect systems in CdF_2:M (M = In, Ga and Al). The calculated oscillator strengths and the refractive index changes are presented.

2. The method of calculation, and the APES of CdF_2:Al

The interaction of the defect electron with the surrounding atoms is described using the one-electron Hartree–Fock approach. The lattice distortion and polarization are treated by the pair potential and Mott and Littleton methods [9]. The APES is determined as a function of the cc chosen (the nearest-neighbour Al^{3+}–F^- distance) by minimizing the total energy of the defect system. The total energy of the system consists of the lattice energy, the energy of the defect electron, and the polarization energy of the crystal. For low concentrations of the dopants, 0.1% or less, the dopant–dopant distance is much larger than the lattice constant. We consider the interaction of the defect electron with a cluster of about 1800 ions surrounding the impurity in calculating the electron energy, and a cluster of about 500 ions for the polarization energy, and about 50 ions are allowed to relax from their perfect-lattice sites during the minimization of the total energy (the relaxation of the ions beyond the third shell makes little contribution to the total energy).

The lattice energy consists of the electrostatic Coulomb energy and the short-range repulsive interaction of the ions. The Coulomb energy is calculated by interpolating the Madelung potential expressed as a series of cubic harmonics (up to the order with $\ell = 8$). And the short-range interaction is represented by a Born–Mayer-type potential:

$$V_{ij} = A_{ij} \exp(-r/\rho_{ij}) \tag{1}$$

for cation–anion pairs (Cd^{2+}–F^-, Al^{3+}–F^-), while for anion–anion pairs, a van der Waals

Table 1. Born–Mayer pair potential coefficients. A, ρ, and C are in atomic units.

Coefficient	Cd^{2+}–F^-	Al^{3+}–F^-	F^-–F^-
A (au)	257.76	54.76	61.90
ρ (au)	0.4641	0.4854	0.5202
C (au)	—	—	23.771

part is included, i.e.,

$$V_{--} = A_{--}\exp(-r/\rho_{--}) - C_{--}/r^6 \tag{2}$$

as the F^-–F^- interaction is apparently attractive at large interionic separation [10]. The interionic potentials were determined by an approach based on the electron gas model of Gordon and Kim [11], and then fitted to the form of the Born–Mayer potential. The short-range repulsive terms are calculated by summing the potentials over the nearest neighbours of the ions being moved. The cation–cation interaction has been excluded since the distance between the positive ions is much larger than the cation–anion separation. The parameters used are listed in table 1.

The same method as in reference [4] has been used to calculate the polarization energy. The polarizabilities used in the present problem are 1.8 $Å^3$ for Cd^{2+} [12], 1.04 $Å^3$ for F^- [12], and 0.351 $Å^3$ for Al^{3+} [13].

The deep-core parameters and extended-ion parameters for Al^{3+} are determined in the same way as described in reference [14]. Three kinds of term are used to represent the outermost-shell electrons of the ions: the overlap integral of the occupied orbitals and the basis functions describing the defect electron, and the screened Coulomb and exchange potentials. The deep-core electrons are described by the so-called ion-size parameters. The defect electron is represented by a linear combination of several floating Gaussian orbitals (FGO) which can describe both diffuse and compact states. We have used one compact and two diffuse Gaussian bases centred on the impurity to represent the defect electron in the s-like ground state. The optimized Gaussian damping factors $\alpha = 0.005$, 0.020, and 0.120 are chosen to treat the defect system CdF_2:Al^{3+}. The most compact basis function here is larger than that used in reference [4] for describing CdF_2:In^{3+} and CdF_2:Ga^{3+}, because the ionic radius of Al^{3+} is much smaller than those of In^{3+} and Ga^{3+}. Other details can be found in reference [4].

The 3s (Al^{3+}) binding energy in the free state is 28.44 eV [15], which is close to that for 5s (In^{3+}), 28.0 eV [15]. As a rough estimate, these values can be reduced by about 20.3 eV, the repulsive Madelung potential in the ionic lattice. Thus, at first sight a state structure similar to that of CdF_2:In^{3+} is expected to appear in CdF_2:Al^{3+}. We calculated the APES of the defect system CdF_2:Al^{3+}, and plotted the results in figure 1(a) (solid line). Here the cc is the nearest Al^{3+}–F^- distance. To our surprise, an unusual bistable-like feature appears. The diffuse state with a small binding energy appears deeper than the compact state which has a large binding energy. In the diffuse state, the lattice strongly 'collapses' toward the impurity Al^{3+}. The first-shell ions surrounding the impurity are displaced by about 0.35 Å from the perfect-lattice sites. The displacements of the second- and third-shell ions are 0.12 Å and 0.14 Å, respectively, which are also large. However, in the compact state, the first shell moves 0.1 Å toward the Al^{3+} ion. The structure is therefore completely different from those in CdF_2:In^{3+} and CdF_2:Ga^{3+}. For the latter, the APES exhibits a shallow diffuse level and a deep compact one, and the lattice relaxation is almost negligible in the deep level. For comparison, we reproduced in figures 1(b) and 1(c) the APES obtained in reference [4].

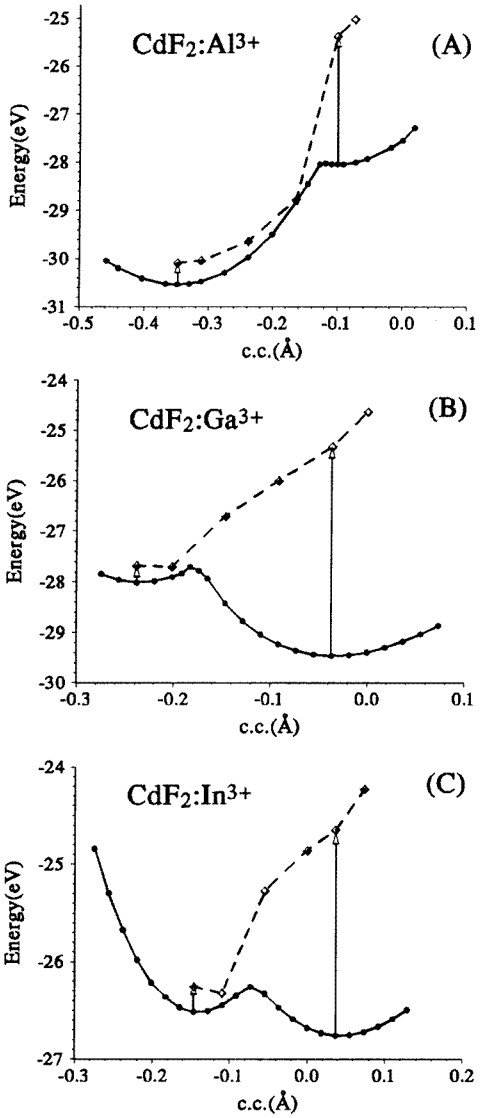

Figure 1. The APES of CdF_2:Al^{3+}, Ga^{3+}, In^{3+}. Solid lines denote the ground states; dashed lines denote the excited p-like states.

From the characteristic data listed in table 2, one can find that the electronic energy for the compact state is -5.52 eV rather than 20.3 eV $-$ 28.44 eV $= -8.14$ eV. This is found to be the result of the effect of the first shell on the correction of the Madelung potential. We notice the relatively large lattice relaxation for the compact state (0.1 Å). In fact, the modified Madelung potential is about 22.6 eV. The resulting electronic energy, 22.6 eV $-$ 28.44 eV $= -5.84$ eV, can then be compared to the purely electronic energy for the compact state, which is -5.52 eV. That is why the expected deep compact level in CdF_2:Al^{3+} rises higher than the diffuse state.

The inward relaxation in the compact state results from the much weaker repulsive

Table 2. Characteristic data for the APES for CdF_2:Al^{3+}.

Distortion (Å)			Energy terms (eV)					Eigenvectors $\{c_i\}$*		
First	Second	Third	Coul.	Rep.	Elec.	Pol.	Total	c_1	c_2	c_3
−0.35	−0.12	−0.14	−26.409	0.964	−2.647	−2.448	−30.540	1.281	0.190	−0.162
−0.13	0.12	0.00	−24.436	0.533	−2.579	−1.562	−28.044	1.490	−0.393	0.523
−0.12	−0.09	−0.06	−21.881	−0.585	−5.038	−0.522	−28.026	−0.515	0.044	−1.417
−0.10	−0.08	−0.05	−21.541	−0.564	−5.523	−0.415	−28.043	−0.425	0.054	−1.456

*The $\{c_i\}$ correspond to the three Gaussian basis functions with α_i respectively equal to 0.005, 0.02, and 0.120.

interaction between Al^{3+} and F^- (see table 1). As the first shell's position reaches the area of the potential barrier (from −0.10 Å to −0.15 Å; see table 2), the displacement of the second shell suddenly changes direction, which causes precipitous changes in the Coulomb energy, the repulsive energy, and the electronic energy. At this point, the defect electron transforms from a localized state (compact) to a diffuse state. The eigenvectors in table 2 show this clearly. We have calculated the APES of CdF_2:Al^{3+} with several different sets of compact bases, and the same features appear in all cases. As there have been no experimental results reported yet, we are not able to make any comparisons at present. However, from the physical point of view, the bistable-like state structure is not unreasonable for the defect system CdF_2:Al^{3+}.

3. Photorefractive properties

Langer and co-workers [1] have presented a qualitative description of the lattice relaxation around the In^{3+} impurity centre in the shallow and deep levels. When an $In^{3+} + e^-$ shallow donor is ionized, the equilibrium configuration does not change; there is no or only a very small difference between the optical and thermal ionization energies for this state. The situation is quite different when the localized In^{3+} state is ionized. The optical and thermal ionization energies are 1.9 eV and 0.25 eV, respectively.

Table 3. Characteristic data for the transition energies, f_{IR}, f_{vis}, and $-\Delta n$

	$\Delta E_{\text{diffuse}}$ (eV)		$\Delta E_{\text{compact}}$ (eV)		f_{IR}		f_{vis}		$-\Delta n$	
	Theor.	Exp.	Theor.	Exp.	Theor.	Based on exp.*	Theor.	Based on exp.*	Theor.	Based on exp.*
In	0.26	0.14	2.11	1.90	0.65	0.35	0.43	0.38	0.70×10^{-4}	0.46×10^{-4}
Ga	0.34	<0.17	4.14	3.00	1.36	0.75	0.19	0.14	1.10×10^{-4}	0.60×10^{-4}
Al	0.45	—	2.45	—	1.27	0.40	0.28	0.20	1.10×10^{-4}	0.40×10^{-4}

*This indicates that the numbers evaluated are obtained using the experimental values of optical transition energies.

To investigate the impurity phototransformation process, we need to calculate the wavefunctions and energies of the ionized states. Generally speaking, theoretical determination of the ionization limit is more complex. One should determine the conduction band edge corresponding to the distorted lattice. Instead we calculated the first p-like state energies at the atomic position corresponding to that of the ground states. Gaussian lobe functions are used to represent the excited p-like state. The excited p-like-state energies are also plotted in figure 1 as dashed lines (the transition energies are listed in table 3).

It is reasonable to assume that, for the shallow state, the ionization limit is quite near the p-like state. However, for the deep compact state this may not be the case. With these qualifications, the excited-state energies are reasonably close to the experimental ionization energies for CdF_2:In^{3+}. For CdF_2:Ga^{3+}, the calculated transition energies, 0.34 eV and 4.14 eV, seem a little large by comparison with the absorption spectra in which two bands peak at 0.17 eV and 4.0 eV, respectively [3]. Overall, however, the trend from CdF_2:In^{3+} to CdF_2:Ga^{3+} is reproduced. The case of CdF_2:Al^{3+} is quite unique, as we have discussed before. Although there are no published data, we feel reasonably confident of our predicted structure.

A two-oscillator model has been employed to estimate the maximum change of the refractive index as has been proposed in [6]:

$$\Delta n = -\frac{r_0 N_{imp}}{2\pi n}\left(\frac{m}{m^*}\right) f_{IR}\lambda^2\left(1+\frac{f_{vis}/f_{IR}}{\lambda^2/\lambda_{vis}^2}\right) \tag{3}$$

where $r_0 = e^2/mc^2 = 2.82\times10^{-13}$ cm, and m/m^* is the electron effective-mass ratio (here it is assumed to be equal to 1, as for CdF_2 the polaron mass does not differ much from the free-electron mass m [8]); f is the value of the oscillator strength of the respective optical absorption; λ and λ_{vis} are the wavelengths of the probe beam and the visible-region absorption, respectively; N_{imp} is the concentration of the donors; and n is the refractive index of the host. The oscillator strength is defined as

$$f_j = \frac{2m}{\hbar^2}\hbar\omega_j|x_{0j}|^2 \tag{4}$$

$$x_{0j} = \int \psi_j^* x \psi_0 \, \mathrm{d}\tau \tag{5}$$

where $\hbar\omega$ is the transition energy.

The calculated results for the oscillator strengths and the refractive index changes $-\Delta n$ are given in table 3. To obtain the data in the columns headed 'Based on exp.' the transition energies are set equal to the experimental data in the calculation. In calculating the index change Δn, we have used $\lambda = 0.5$ μm, $N_{imp} = 10^{18}$ cm^{-3}, and $n = 1.5$, as in references [6, 7].

The present work gives an oscillator strength of about 0.14–1.36, which is close to the range inferred from experiment [1, 8]. More interestingly, the refractive index change induced by the optical process is about 10^{-4}, which is in the same range as values reported in references [6, 7]. The optical process employed in holographic recording is briefly as follows. At temperatures low enough that the defects are in their stable states (e.g. the deep compact state for CdF_2:In^{3+}, Ga^{3+}), optical ionization with about 3 eV (for In) and 4 eV (for Ga) photons takes the electrons successively to the compact ionized state, then to the diffuse ionized state via non-radiative transitions, and finally to the metastable shallow donor state. This cycle induces the refractive index change which we have evaluated. Below about 100 K and 260 K respectively for In^{3+} and Ga^{3+} centres, the metastable shallow state can be preserved, thereby storing the optical data.

Whether a similar process is possible in CdF_2:Al^{3+} is obviously an interesting question. From the APES obtained, and especially because of the large energy difference between the stable diffuse state and the metastable compact state, a similar process seems impossible to realize.

Acknowledgment

The authors would like to thank Professor J M Langer for the interest shown in their work.

References

[1] Piekara U, Langer J M and Krukowska-Fulde B 1977 *Solid State Commun.* **23** 583
Dmochowski J E, Langer J M, Kalinski Z and Jantsch W 1986 *Phys. Rev. Lett.* **56** 1735
[2] Langer J M 1980 *New Developments in Semiconductor Physics (Springer Lecture Notes in Physics 122)* (New York: Springer) p 123
Langer J M 1980 *J. Phys. Soc. Japan Suppl.* A **49** 207
Langer J M 1983 *Radiat. Eff.* **27** 55
[3] Dmochowski J E, Jantsch W, Dobosz D and Langer J M 1988 *Acta. Phys. Pol.* **73** 247
[4] Cai Yang and Song K S 1995 *J. Phys.: Condens. Matter* **7** 2275
[5] Eisenberger P and Pershan P S 1968 *Phys. Rev.* **167** 292
[6] Ryskin A L, Shcheulin A S, Koziarska B, Langer J M, Suchocki A, Buczinskaya I I, Fedorov P P and Sobolev B P 1995 *Appl. Phys. Lett.* **67** 31
[7] Koziarska B, Langer J M, Ryskin A I, Shcheulin A S and Suchocki A 1995 *Acta. Phys. Pol.* **88** 1010
[8] Langer J M, Langer T, Pearson G L, Krukowska-Fulde B and Piekara U 1974 *Phys. Status Solidi* b **66** 537
[9] Mott N F and Littleton M J 1938 *Trans. Faraday Soc.* **34** 485
[10] Norgett M J 1971 *J. Phys. C: Solid State Phys.* **4** 298
Norgett M J 1971 *J. Phys. C: Solid State Phys.* **4** 1284
[11] Gordon R G and Kim Y S 1972 *J. Chem. Phys.* **56** 3122
[12] Tessman J R, Kahn A H and Shockley W 1953 *Phys. Rev.* **92** 890
[13] Pauling L 1927 *Prog. R. Soc.* A **114** 181
[14] Song K S and Williams R T 1996 *Self-Trapped Excitons* 2nd edn (Berlin: Springer)
[15] Moore C E 1971 *Atomic Energy Levels* vol 1, NBS Circular (Washington, DC: US Government Printing Office) (reissued)